

# OmniEdit: A Training-free framework for Lip Synchronization and Audio-Visual Editing

Lixiang Lin<sup>1</sup>, Siyuan Jin<sup>2\*</sup>, and Jinshan Zhang<sup>3</sup>

<sup>1</sup> HiThink Research

linlixiang@myhexin.com

<sup>2</sup> University of Science and Technology of China

<sup>3</sup> Zhejiang University

**Abstract.** Lip synchronization and audio-visual editing have emerged as fundamental challenges in multimodal learning, underpinning a wide range of applications, including film production, virtual avatars, and telepresence. Despite recent progress, most existing methods for lip synchronization and audio-visual editing depend on supervised fine-tuning of pre-trained models, leading to considerable computational overhead and data requirements. In this paper, we present OmniEdit, a training-free framework designed for both lip synchronization and audio-visual editing. Our approach reformulates the editing paradigm by substituting the edit sequence in FlowEdit with the target sequence, yielding an unbiased estimation of the desired output. Moreover, by removing stochastic elements from the generation process, we establish a smooth and stable editing trajectory. Extensive experimental results validate the effectiveness and robustness of the proposed framework. Code is available at <https://github.com/l1346792580123/OmniEdit>.

**Keywords:** Training-free · Lip synchronization · Audio-visual editing

## 1 Introduction

Lip synchronization [18, 31, 33, 43], which aims to align mouth movements with corresponding speech audio, is a fundamental yet critical task in computer vision. By enforcing fine-grained temporal and semantic consistency between facial dynamics and acoustic signals, lip synchronization plays an essential role in applications such as film dubbing and digital human generation. As a result, it has become a foundational component in modern video generation systems, underpinning the realism and perceptual quality of AI-generated visual content.

Audio-visual editing [4, 20, 21], whose goal is to simultaneously manipulate visual content and corresponding audio signals according to textual prompts, can be seen as an advanced extension of lip synchronization. Unlike lip synchronization, which focuses primarily on aligning mouth movements with speech, audio-visual editing requires coherent cross-modal modifications, preserving semantic consistency and temporal alignment across both visual and auditory

---

\* work done during internship at HiThink Research.

streams, thereby enabling more flexible and expressive multimodal content generation.

With the rapid advancement of diffusion-based generative models [12, 22, 32, 34], numerous lip synchronization approaches have been developed by performing supervised fine-tuning on text-to-image or text-to-video models. These methods typically require the collection of large-scale paired audio-visual datasets to learn accurate cross-modal alignment. Moreover, they often rely on explicit mouth-region masking or incorporate specialized training strategies to enforce fine-grained correspondence between speech signals and lip movements, thus increasing both data and computational demands.

Audio-visual editing similarly relies on paired audio-visual data, which are scarce and difficult to collect, for supervised fine-tuning. Alternatively, it often depends on computationally intensive optimization-based approaches. These requirements pose significant obstacles to progress in the field and limit the feasibility of deploying such techniques in practical applications.

Motivated by the limitations discussed above, we propose OmniEdit, a training-free framework specifically designed for lip synchronization and audio-visual editing. Leveraging pre-trained audio-to-video diffusion models and audio-visual foundation models, our approach enables precise lip synchronization and supports rich, flexible audio-visual editing without requiring task-specific fine-tuning or large-scale paired datasets.

We first replace the iterative refinement of the edit sequence in FlowEdit [17] with iterations over the target sequence, obtaining an unbiased estimate of the desired output. This reformulation not only reduces the inherent bias introduced by sequential editing but also enables a more direct alignment with the target distribution.

Second, we eliminate the stochastic Gaussian sampling in the generation process and replace it with noise estimated by the pre-trained diffusion model, hence constructing a smoother iterative trajectory that enhances both the stability and quality of the generated results.

Our contributions can be summarized as follows:

- We present **OmniEdit**, the first training-free framework for lip synchronization and audio-visual editing, eliminating the need for task-specific fine-tuning, and paving the way for plug-and-play multimodal content creation.
- We establish a target iterative sequence to enable an unbiased estimation of the desired output, reducing bias from sequential editing and facilitating more direct alignment with the target distribution.
- We construct a deterministic and smooth generation trajectory by replacing stochastic Gaussian sampling with semantically consistent noise estimated from a pre-trained diffusion model to enhance output quality.
- OmniEdit achieves state-of-the-art performance without additional training, rivaling or surpassing supervised methods in lip synchronization while supporting flexible cross-modal audio-visual editing.

## 2 Related Works

### 2.1 Omni-Modal Generation

**Audio-driven video generation** is commonly categorized into lip synchronization and portrait animation, distinguished primarily by their input settings. Lip synchronization operates on a given video to match target audio, while portrait animation generates video content using only audio and a reference image. Early GAN-based [7] methods [2, 26, 33, 41] provided fundamental advances that shaped subsequent developments in lip synchronization. The emergence of diffusion models [18, 25, 31, 43] has markedly advanced the state of the art in audio-driven lip synchronization. Omnisync [31] adopts a mask-free training strategy with diffusion transformer models, allowing direct frame-level editing in the absence of explicit masking. Despite achieving promising results, the approach still requires additional training or model fine-tuning.

Portrait Animation [1, 3, 5, 6, 13, 28, 38] differs from lip synchronization in that it directly generates videos by driving a reference image with an audio signal. While this approach requires fewer conditional inputs, it typically offers limited control over background, head pose, and detailed facial expressions. We propose a training-free method that leverages a portrait animation model to achieve lip synchronization, hence unifying the two approaches.

**Audio-Visual Generation** refers to the task of jointly synthesizing synchronized video and audio from a single text prompt. Ovi [24] and BridgeDiT [8] enable simultaneous audio-visual generation by integrating existing text-to-video (T2V) and text-to-audio (T2A) architectures, which often leads to high computational overhead and limited cross-modal synergy. LTX-2 [9] employs a decoupled dual-stream architecture with asymmetric design and bidirectional cross-attention, enabling robust audio-visual alignment with substantially lower computational overhead.

### 2.2 Training Free Editing

Training-free editing has emerged as an important direction in diffusion-based generative modeling, as it enables image manipulation without requiring additional model retraining or task-specific fine-tuning. Optimization-based editing [10, 15, 16, 30] directly modifies the input image by iteratively optimizing it toward consistency with a given textual prompt. Inversion-based editing [11, 35, 39, 40] involves recovering a noise map via image-to-noise inversion and subsequently applying the conventional diffusion process guided by the target prompts to achieve the intended modifications.

FlowEdit [17] introduces an inversion-free, optimization-free and model agnostic method for text-based image editing. FlowEdit constructs a direct ODE between the source and target distributions, without passing through the standard Gaussian distribution. FlowAlign [14] extends FlowEdit by promoting a smoother transition from source to target. FlowDirector [19] further introduces flow correction and applies the framework to text-to-video editing.

### 3 Preliminaries

#### 3.1 Flow Matching

Flow Matching [22] is a framework for learning continuous-time generative models by directly regressing the vector field of a probability flow. The transportation between the data distribution  $X_0$  and the Gaussian distribution  $X_1 \sim \mathcal{N}(0, I)$ , is defined by an ordinary differential equation (ODE)

$$dX_t = V(X_t, t)dt, \quad (1)$$

$t \in [0, 1]$ ,  $V$  is the velocity field. Flow matching trains a neural network  $v_\theta$  to model the velocity field by minimizing

$$\mathcal{L}_{FM} = \mathbb{E} \|v_\theta(x_t, t) - V(x_t, t|x_1)\|^2, \quad (2)$$

where  $x_t \sim X_t, x_1 \sim X_1$ ,  $V(x_t, t|x_1)$  is the conditional velocity field. Once  $v_\theta$  is trained, the data sample can be generated by sampling a random Gaussian noise and solving the ODE iteratively.

Rectified Flow [23] is a particular instantiation of flow matching that constructs a linear interpolation path between samples from the data distribution and the Gaussian distribution  $x_t = (1-t)x_0 + tx_1$ , resulting in a constant target velocity  $V(x_t, t|x_1) = x_1 - x_0$  that transports noise to data along straight-line trajectories.

For conditional generation, the velocity field is parameterized to depend on auxiliary conditioning information, such as text or audio. Conditional generative flow models are trained on paired observations of data and conditions, enabling sampling from the corresponding conditional data distribution.

#### 3.2 FlowEdit

FlowEdit [17] presents an inversion-free and model agnostic method for text-based image editing using pretrained flow models. FlowEdit reinterprets inversion as a direct path between the source and target distribution, and defines an edit sequence

$$X_t^{edit} = X^{src} + X_t^{tar} - X_t^{src}, \quad (3)$$

$$X_t^{src} = (1-t)X^{src} + t\epsilon. \quad (4)$$

$X^{src}$  is the source image,  $\epsilon \sim \mathcal{N}(0, I)$  is Gaussian noise,  $X_t^{src}$  and  $X_t^{tar}$  represent the inversion sequence and forward sequence of source image and target image respectively.  $X_t^{src}$  is constructed by adding Gaussian noise to the source image, and  $X_t^{tar}$  is computed according to Eq. 3  $X_t^{tar} = X_t^{edit} - X_t^{src} + X^{src}$ . The transportation ODE of  $X_t^{edit}$  is defined by

$$dX_t^{edit} = (V(X_t^{tar}, t) - V(X_t^{src}, t))dt. \quad (5)$$

For more details, we suggest readers to refer to the FlowEdit [17] paper.

While FlowEdit defines the direct transportation from source image to target image, making the iteration results noise-free, some problems still exist. First, the editing process starts from  $t_{max}$  instead of 1, and  $X_{t_{max}}^{edit}$  is initialized to  $X^{src}$ . Consequently, the resulting edited output is not strictly equivalent to the desired target sample  $X^{tar}$ . Instead, it is given by

$$X^{edit} = X^{src} + \int_{t_{max}}^0 (V(X_t^{tar}, t) - V(X_t^{src}, t))dt, \quad (6)$$

which reveals that the final estimate depends on the discrepancy between the target and source velocity fields accumulated along the truncated trajectory. This mismatch between the initialization scheme and the ideal diffusion boundary condition introduces an inherent bias in the editing process, preventing exact recovery of the target distribution.

One may consider initializing the process from  $t = 1$  to better align with the full diffusion formulation. However, doing so would substantially increase computational cost due to the extended integration horizon. Moreover, starting from pure Gaussian noise at  $t = 1$  tends to degrade the fidelity of the final result, as the trajectory must traverse a longer path from an information-free state, making it more susceptible to accumulated numerical errors and instability during generation.

Second, as noted in FlowAlign [14], sampling a random Gaussian noise  $\epsilon_t$  at each iteration to generate  $x_t^{src}$  produces a non-smooth trajectory. This temporal inconsistency propagates to  $x_t^{edit}$ , reducing optimization stability, increasing computational overhead, and hindering the attainment of optimal performance.

## 4 OmniEdit

Motivated by the above issues, we introduce OmniEdit, a training-free framework designed for lip synchronization with concurrent audio-visual editing capabilities. Fig 1 shows the overview of the framework. We reformulate the FlowEdit paradigm by replacing the conventional iterative edit sequence with an iteration scheme defined directly over the target sequence. Furthermore, we remove stochastic sampling from the editing process.

We begin by presenting the formulation of the proposed target-sequence iteration strategy and detailing how stochastic sampling can be systematically removed from the editing pipeline. Building upon this unified framework, we further demonstrate its applicability to both lip synchronization and audio-visual editing tasks, showing that the same formulation can accommodate precise mouth-motion alignment as well as broader multimodal content manipulation in a coherent and consistent manner.

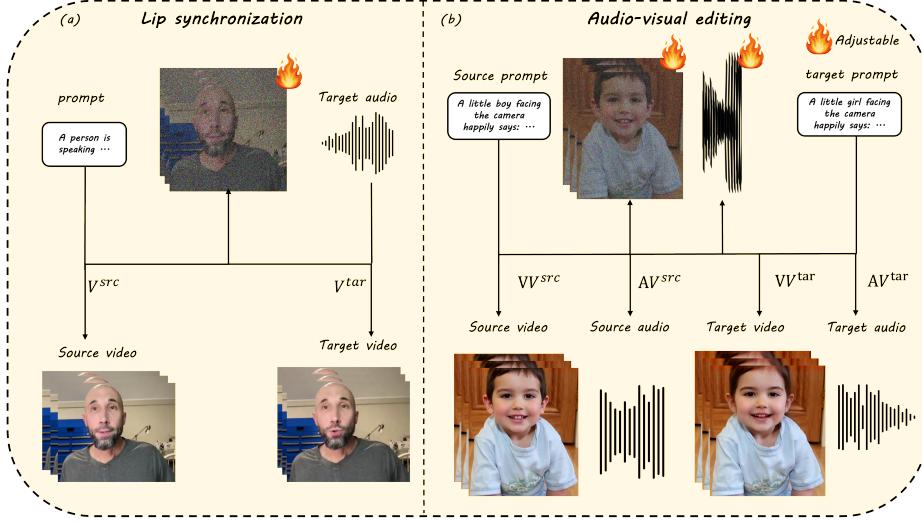


**Fig. 1: Overview of OmniEdit.** (a) Conditioned on the target audio, OmniEdit leverages a pre-trained audio-to-video diffusion signal to synchronize the lip movements in the source video with the target audio signal. (b) Utilizing an audio-visual generation model, OmniEdit performs concurrent modification of audio and video modalities according to target prompt.

#### 4.1 Target Sequence Iteration

We reframe the FlowEdit iteration process, transforming the iteration sequence of the edit sequence into the iteration of the target sequence

$$X_{t_{max}}^{tar} = X_{t_{max}}^{src} = (1 - t_{max})X^{src} + t_{max}\epsilon, \quad (7)$$

$$X_{t_i}^{tar} = X_{t_i}^{edit} - X_{t_i}^{src} + X^{src}, \quad (8)$$

$$\begin{aligned} X_{t_{i-1}}^{tar} &= X_{t_i}^{tar} + X_{t_{i-1}}^{edit} - X_{t_i}^{edit} + X_{t_{i-1}}^{src} - X_{t_i}^{src} \\ &= X_{t_i}^{tar} + (t_{i-1} - t_i)(V_{t_i}^{tar} - V_{t_i}^{src}) + X_{t_{i-1}}^{src} - X_{t_i}^{src}. \end{aligned} \quad (9)$$

$\{t_i\}_{i=0}^T$  is a monotonically decreasing time schedule.  $X_{t_{max}}^{tar}$  and  $X_{t_{max}}^{src}$  are initialized by adding the same Gaussian noise in  $X^{src}$ . The continuous-time ODE of the edit sequence in Eq. 5 is solved using a numerical ODE solver via time discretization.

In contrast to the edit sequence, the target sequence yields an unbiased estimate of the desired target quantity. Specifically, the initialization of the target trajectory is defined as  $X_{t_{max}}^{tar} = (1 - t_{max})X^{src} + t_{max}\epsilon$ . By comparison, the edit sequence is initialized directly from the clean source input,  $X_{t_{max}}^{edit} = X^{src}$ . This discrepancy between the actual initial state and the theoretically prescribed terminal state results in a systematic mismatch, which introduces bias into the estimation obtained through the edit sequence.

By reformulating the iterative process in terms of the target sequence, we obtain a clearer interpretation of the underlying dynamical system and improve its analytical tractability. This reformulation not only facilitates theoretical analysis of the iteration dynamics but also provides a more principled foundation for the design of the associated noise parameterization.

## 4.2 Random Noise Elimination

Eq. 9 can be further reformulated into the following form

$$X_{t_{i-1}}^{tar} = X_{t_i}^{tar} + (t_{i-1} - t_i)V_{t_i}^{tar} + X_{t_{i-1}}^{src} - (X_{t_i}^{src} + (t_{i-1} - t_i)V_{t_i}^{src}), \quad (10)$$

which can be interpreted as augmenting the iteration of the target sequence with the incremental variation induced by the source sequence iteration. This further indicates that the introduction of random noise into the source sequence in FlowEdit [17] is suboptimal, since it leads to irregular trajectories and increases the iterative error of the source sequence.

Inspired by Noise-Level Guidance [27] and FlowCycle [42], the initial random noise in the diffusion process can significantly influence the final output, leading to variations in image quality and prompt adherence. We replace the random noise injection in FlowEdit with an estimated noise formulation. Specifically,  $X_{t_{i-1}}^{src}$  is no longer initialized from randomly sampled noise, but instead derived from the noise estimated at the previous iteration

$$\hat{\epsilon}_{t_{i-1}} = X_{t_i}^{src} + (1 - t_i)V_{t_i}^{src}, \quad (11)$$

$$X_{t_{i-1}}^{src} = (1 - t_{i-1})X^{src} + t_{i-1}\hat{\epsilon}_{t_{i-1}}. \quad (12)$$

By adopting this modification, we obtain smoother iteration dynamics and alleviate error accumulation associated with random noise.

## 4.3 Lip Synchronization

The proposed method can be directly applied to a pre-trained audio-to-video diffusion model for accurate lip synchronization. By incorporating the aforementioned theoretical analysis into the inference process, we can enable precise audio-lip alignment while preserving the pre-trained model’s generalization ability and expressive capacity.

Algorithm 1 outlines the proposed OmniEdit procedure for audio-driven lip synchronization within a training-free generative flow framework. Given a source video  $X^{src}$ , a predefined time schedule  $\{t_i\}_{i=0}^T$ , and a pretrained audio-driven video generation diffusion model  $V_\theta$ , the method synthesizes a target video  $X^{tar}$  that preserves the visual identity and dynamics of the source while conforming to a target audio signal  $A^{tar}$ .

The algorithm begins by estimating a Gaussian noise and constructing the initial noisy target state  $X_{t_{max}}^{tar} = (1 - t_{max})X^{src} + t_{max}\epsilon$  via linear interpolation between the source video and noise. The procedure then iteratively traverses the

**Algorithm 1: OmniEdit for Lip Synchronization**


---

**Input:** source video  $X^{src}$ ,  $\{t_i\}_{i=0}^T$ , pretrained model  $V_\theta$ , prompt  $c$   
 $n_{max}$ , target audio  $A^{tar}$ , source audio  $A^{src}$  (optional)  
**Output:** target video  $X^{tar}$   
**if**  $A^{src}$  *is missing* **then**  
  |  $\epsilon \leftarrow \mathcal{N}(0, I)$   
**else**  
  |  $\epsilon \leftarrow V_\theta(X^{src}, A^{src}, 0, c) + X^{src}$   
**end**  
 $X_{t_{max}}^{tar} \leftarrow (1 - t_{max})X^{src} + t_{max}\epsilon$   
**for**  $i = n_{max}$  **to** 0 **do**  
  |  $X_{t_i}^{src} \leftarrow (1 - t_i)X^{src} + t_i\epsilon$   
  | **if**  $A^{src}$  *is missing* **then**  
  | |  $V_{t_i}^{src} \leftarrow V_\theta(X_{t_i}^{src}, A^{null}, t_i, c)$   
  | **else**  
  | |  $V_{t_i}^{src} \leftarrow V_\theta(X_{t_i}^{src}, A^{src}, t_i, c)$   
  | **end**  
  |  $V_{t_i}^{tar} \leftarrow V_\theta(X_{t_i}^{tar}, A^{tar}, t_i, c)$   
  |  $\epsilon \leftarrow X_{t_i}^{src} + (1 - t_i)V_{t_i}^{src}$   
  |  $X_{t_{i-1}}^{src} \leftarrow (1 - t_{i-1})X^{src} + t_{i-1}\epsilon$   
  |  $X_{t_{i-1}}^{tar} \leftarrow X_{t_i}^{tar} + (t_{i-1} - t_i)(V_{t_i}^{tar} - V_{t_i}^{src}) + X_{t_{i-1}}^{src} - X_{t_i}^{src}$   
**end**  
**Return:**  $X_0^{tar}$

---

discretized time steps in reverse order. At each step  $t_i$ ,  $X_{t_i}^{src}$  is constructed using the adjustable variable  $\epsilon$ , which is updated following the derivation in Sec. 4.1. The pretrained model  $V_\theta$  predicts the velocity fields conditioned on the available audio signals. When the source audio  $A^{src}$  is absent, a null condition is used to maintain compatibility, just like unconditional inference. For simplicity, we omit the classifier-free guidance in the  $V_{t_i}^{tar}$  computation. By repeatedly applying these coupled updates, the algorithm progressively refines the target video along the reverse flow, yielding the final synchronized output  $X^{tar}$ .

#### 4.4 Audio-Visual Editing

Similarly, by leveraging a pre-trained audio-visual foundation model, OmniEdit extends naturally to prompt-driven audio-visual editing. Textual prompts serve as high-level semantic guidance, enabling coherent manipulation of both visual and auditory modalities.

Algorithm 2 details the overall procedure for joint audio-visual editing. In contrast to Algorithm 1, this formulation incorporates source prompt  $c^{src}$  and target prompt  $c^{tar}$  as input and produces a corresponding target audio signal  $A^{tar}$  alongside the edited video. Under the guidance of the specified prompt, the framework simultaneously performs visual and auditory modifications, ensuring that both the generated target video and audio are coherently aligned with the intended semantic and perceptual attributes.

**Algorithm 2:** OmniEdit for Audio-Visual Editing

---

**Input:** source video  $X^{src}$ ,  $\{t_i\}_{i=0}^T$ , pretrained model  $V_\theta$ ,  $n_{max}$ , source prompt  $c^{src}$ , target prompt  $c^{tar}$ , source audio  $A^{src}$  (optional)  
**Output:** target video  $X^{tar}$ , target audio  $A^{tar}$

**if**  $A^{src}$  *is missing* **then**

- $\epsilon^{init} \sim \mathcal{N}(0, I)$ ,  $A_T^{src} \leftarrow \epsilon^{init}$ ,  $A_T^{tar} \leftarrow \epsilon^{init}$
- for**  $i = T$  **to**  $n_{max}$  **do**
  - $\epsilon \sim \mathcal{N}(0, I)$
  - $X_{t_i}^{src} \leftarrow (1 - t_i)X^{src} + t_i\epsilon$
  - $X_{t_i}^{tar} \leftarrow (1 - t_i)X^{src} + t_i\epsilon$
  - $AV_{t_i}^{src}, VV_{t_i}^{src} \leftarrow V_\theta(X_{t_i}^{src}, A_{t_i}^{src}, t_i, c^{src})$
  - $AV_{t_i}^{tar}, VV_{t_i}^{tar} \leftarrow V_\theta(X_{t_i}^{tar}, A_{t_i}^{tar}, t_i, c^{tar})$
  - $A_{t_{i-1}}^{src} \leftarrow A_{t_i}^{src} + (t_{i-1} - t_i)AV_{t_i}^{src}$
  - $A_{t_{i-1}}^{tar} \leftarrow A_{t_i}^{tar} + (t_{i-1} - t_i)AV_{t_i}^{tar}$
- end**

**else**

- $AV^{init}, VV^{init} \leftarrow V_\theta(X^{src}, A^{src}, 0, c^{src})$
- $\epsilon^{audio}, \epsilon^{video} \leftarrow AV^{init} + A^{src}, VV^{init} + X^{src}$
- $A_{t_{max}}^{src} \leftarrow (1 - t_{max})A^{src} + t_{max}\epsilon^{audio}$
- $A_{t_{max}}^{tar} \leftarrow (1 - t_{max})A^{src} + t_{max}\epsilon^{audio}$

**end**

**for**  $i = n_{max}$  **to** 0 **do**

- $X_{t_i}^{src} \leftarrow (1 - t_i)X^{src} + t_i\epsilon$
- $AV_{t_i}^{src}, VV_{t_i}^{src} \leftarrow V_\theta(X_{t_i}^{src}, A_{t_i}^{src}, t_i, c^{src})$
- $AV_{t_i}^{tar}, VV_{t_i}^{tar} \leftarrow V_\theta(X_{t_i}^{tar}, A_{t_i}^{tar}, t_i, c^{tar})$
- $\epsilon^{audio} \leftarrow A_{t_i}^{src} + (1 - t_i)AV_{t_i}^{src}$
- $\epsilon^{video} \leftarrow X_{t_i}^{src} + (1 - t_i)VV_{t_i}^{src}$
- $X_{t_{i-1}}^{src} \leftarrow (1 - t_{i-1})X^{src} + t_{i-1}\epsilon^{video}$
- $X_{t_{i-1}}^{tar} \leftarrow X_{t_i}^{tar} + (t_{i-1} - t_i)(VV_{t_i}^{tar} - VV_{t_i}^{src}) + X_{t_{i-1}}^{src} - X_{t_i}^{src}$
- if**  $A^{src}$  *is missing* **then**
  - $A_{t_{i-1}}^{src} \leftarrow A_{t_i}^{src} + (t_{i-1} - t_i)AV_{t_i}^{src}$
  - $A_{t_{i-1}}^{tar} \leftarrow A_{t_i}^{tar} + (t_{i-1} - t_i)AV_{t_i}^{tar}$
- else**
  - $A_{t_{i-1}}^{src} \leftarrow (1 - t_i)A^{src} + t_{i-1}\epsilon^{audio}$
  - $A_{t_{i-1}}^{tar} \leftarrow A_{t_i}^{tar} + (t_{i-1} - t_i)(AV_{t_i}^{tar} - AV_{t_i}^{src}) + A_{t_{i-1}}^{src} - A_{t_i}^{src}$
- end**

**end**

**Return:**  $A_0^{tar}, X_0^{tar}$

---

When both the source video and source audio are available, Algorithm 2 can be seen as an extension of Algorithm 1 that incorporates the audio modality and updates the target audio sequence along with the corresponding audio noise. However, when source audio is missing,  $A_T^{src}$  and  $A_T^{tar}$  are initialized with the same noise realization. To obtain results corresponding to the desired noise level, both variables undergo iterative denoising from step  $T$  to  $n_{max}$ . The same iterative denoising procedure is applied during the editing stage. This design

**Table 1:** Quantitative results on HDTF Dataset.

Methods	Full Reference Metrics			No Reference Metrics			Lip Sync	
	FID↓	FVD↓	CSIM↑	NIQE↓	BRISQUE↓	HyperIQA↑	LMD↓	LSE-C↑
Wav2Lip [33]	14.912	543.340	0.852	6.495	53.372	45.822	10.007	7.630
IP-LAP [45]	9.512	325.691	0.809	6.533	54.402	50.086	7.695	7.260
Diff2Lip [29]	12.079	461.341	0.869	6.261	49.361	48.869	18.986	7.140
MuseTalk [43]	8.759	231.418	0.862	5.824	46.003	55.397	8.701	6.890
LatentSync [18]	8.518	216.899	0.859	6.270	50.861	53.208	17.344	<b>8.050</b>
Omnisync [31]	7.855	199.627	0.875	5.481	37.917	<b>56.356</b>	<b>7.097</b>	7.309
Ours(Humo1.7B)	7.952	201.038	0.879	5.604	39.527	54.714	7.698	7.157
Ours(Humo17B)	<b>7.623</b>	<b>190.299</b>	<b>0.883</b>	<b>5.385</b>	<b>37.412</b>	55.973	7.482	7.286

**Table 2:** Quantitative results on AIGC-LipSync Benchmark.

Methods	Full Reference Metrics			No Reference Metrics			Generation Success Rate	
	FID↓	FVD↓	CSIM↑	NIQE↓	BRISQUE↓	HyperIQA↑	All Videos↓	Stylized Characters↑
Wav2Lip [33]	22.989	562.245	0.727	5.392	42.816	50.511	71.38%	26.67%
IP-LAP [45]	14.686	247.402	0.796	5.546	45.153	53.174	45.53%	6.67%
Diff2Lip [29]	23.542	403.149	0.692	5.440	42.442	50.335	74.63%	36.67%
MuseTalk [43]	17.668	297.621	0.667	4.935	36.017	58.334	92.20%	67.78%
LatentSync [18]	15.374	263.111	0.751	5.342	41.917	54.648	74.96%	35.56%
Omnisync [31]	10.681	211.350	0.808	4.588	25.485	<b>61.906</b>	<b>97.40%</b>	<b>87.78%</b>
Ours(Humo1.7B)	10.516	213.136	0.824	4.632	26.374	56.215	96.26%	79.98%
Ours(Humo17B)	<b>9.663</b>	<b>203.335</b>	<b>0.831</b>	<b>4.370</b>	<b>23.856</b>	58.621	96.75%	84.27%

not only produces audio consistent with the target video but also enables audio dubbing of the source video conditioned on the source prompt.

Owing to the inherent interdependence between audio and visual modalities in audio–visual generative models, OmniEdit may be naturally extended to cross-modal generation tasks, such as synthesizing video from audio or generating audio from video. Leveraging the unified target-sequence formulation, these extensions could enable coherent and semantically consistent cross-modal content generation, further broadening the framework’s applicability. We consider such extensions to be promising directions for future work.

## 5 Experiments

### 5.1 Experimental Setups

We utilize Humo [1] for lip synchronization and LTX-2 [9] for audio–visual editing. Humo is a unified human-centric framework for video generation that enables audio-driven synthesis and facilitates collaborative control across multiple modalities. LTX-2 is an open-source foundational model enabling joint generation of audio and video, producing temporally synchronized content in a unified



**Fig. 2: Qualitative results** of our proposed method and other methods. Our method achieves more accurate lip synchronization and produces clearer dental details. Please zoom in to observe the fine-grained improvements.

manner. For Humo, the total number of denoising steps is set to 20, with an initial step of 6. For LTX-2, we employ 40 total denoising steps and an initial step of 12. We evaluate lip synchronization using quantitative and qualitative metrics, while audio-visual editing is qualitatively assessed in the absence of a corresponding benchmark.

## 5.2 Lip Synchronization

We compare OmniEdit with OmniSync [31], LatentSync [18], MuseTalk [43], IP-LAP [45], Diff2Lip [29], and Wav2Lip [33] on HDTF [44] dataset and AIGC-LipSync Benchmark. We follow the same evaluation metrics and datasets as OmniSync. Visual quality is evaluated using FID (Fréchet Inception Distance), FVD (Fréchet Video Distance), and CSIM (Cosine Similarity). We additionally report no-reference perceptual metrics, including NIQE (Natural Image Quality

**Table 3: Ablation study** for our proposed method.

Methods	FID↓	FVD↓	CSIM↑	NIQE↓	BRISQUE↓	HyperIQA↑	LSE-C↑
Edit sequence	7.944	198.409	0.878	5.408	37.526	55.198	7.284
Random noise	7.707	194.916	0.880	5.396	37.457	55.492	7.286
Ours	7.623	190.299	0.883	5.385	37.412	55.973	7.286

Evaluator), BRISQUE (Blind/Referenceless Image Spatial Quality Evaluator), and HyperIQA [36]. Audio-visual synchronization performance is measured via LMD (Landmark Distance), and LSE-C (Lip Sync Error – Confidence).

We evaluate Generation Success Rate (GSR) on the AIGC-LipSync benchmark for both the full set and stylized characters. The GSR quantifies the proportion of videos exhibiting correct lip synchronization as confirmed by human evaluators, providing a crucial metric for assessing the effectiveness of universal lip synchronization in AI-generated content.

The experimental results on the HDTF dataset are presented in Tab. 1. Our method achieves comparable performance to the current state-of-the-art approach, OmniSync. By formulating lip synchronization as an editing process, our approach minimally alters the original video while maximally preserving identity consistency, resulting in the lowest FID and FVD scores, as well as the highest CSIM. Regarding no-reference quality metrics, our method outperforms OmniSync in terms of NIQE and BRISQUE, while achieving slightly lower performance on HyperIQA. In terms of lip-synchronization-specific metrics, including LMD and LSE-C, our method performs slightly worse than OmniSync.

The quantitative results on the AIGC-LipSync Benchmark are shown in Tab. 2. Our method again achieves the lowest FID and FVD scores, together with the highest CSIM, demonstrating its strong capability in preserving visual quality and identity consistency. In terms of generation success rate, our approach performs slightly worse than OmniSync. This limitation can be attributed to Humo, which is primarily trained on human-centric datasets and thus exhibits a relatively lower driving success rate on stylized characters. Nevertheless, our method still outperforms other methods in this regard.

The qualitative results are illustrated in Fig. 2. The results of omnisynt come from Kling’s website [37]. Our method achieves more precise lip synchronization while rendering sharper and more detailed dental structures. Moreover, it effectively handles challenging scenarios, such as occlusions and profile views, demonstrating strong robustness under complex conditions. Comprehensive visual results are provided in the github page.

### 5.3 Ablation Study

To validate the contribution of each component in our framework, we conduct an ablation study on key modules, including replacing the edit sequence with the target sequence and removing stochastic noise from the generation process.



**Fig. 3: Ablation study** for edit sequence and random noise. Edit sequence and stochastic noise injection tends to produce blurred dental details, whereas our method is capable of generating sharper and more clearly defined teeth.

Quantitative results are reported in Tab. 3, and qualitative comparisons are presented in Fig. 3.

Although the iterative process over the edit sequence can produce noise-free results, it fails to yield an unbiased estimate of the target, which consequently degrades the fidelity and visual clarity of the generated results. In contrast, iterating over the target sequence more accurately approximates the underlying ODE, leading to improved generative quality as reflected by lower FID and FVD scores. As illustrated in Fig. 3, iterating over the edit sequence produces noticeably blurred teeth, whereas the target-sequence iteration yields significantly sharper and more clearly defined dental details.

Similarly, introducing randomly sampled Gaussian noise when computing the source sequence yields a non-smooth iterative trajectory, which adversely affects generation quality and leads to higher FID and FVD scores. In contrast, replacing stochastic noise with estimated noise produces a smoother trajectory, thereby improving the overall quality of the generated results. As shown in Fig. 3, incorporating random noise also results in degraded visual clarity, particularly in the dental region, while our approach preserves sharper structural details and achieves superior overall quality.

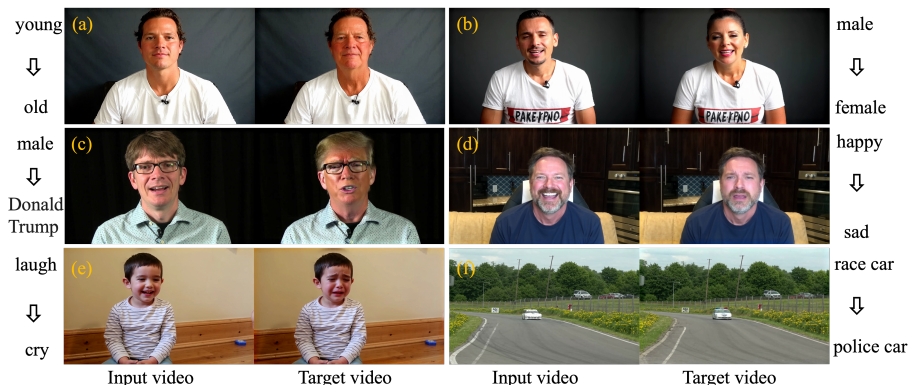


**Fig. 4: Qualitative results of OmniEdit for Audio-visual Editing.** Our approach supports prompt-based manipulation of diverse attributes—including age (a), gender (b), person (c), emotion (d), behaviors (e), and even car categories (f), while jointly generating audio and video in a temporally synchronized and semantically consistent manner.

#### 5.4 Audio-Visual Editing

Due to the absence of a standardized benchmark for audio-visual editing, we conduct a qualitative evaluation of OmniEdit to assess its performance in this setting. As illustrated in Fig. 4, our proposed method demonstrates the ability to modify input videos according to given textual prompts, enabling controlled editing of attributes such as age, gender, identity, emotion, behaviors, and car categories. These results highlight the flexibility and generality of OmniEdit in handling diverse and semantically rich audio-visual editing tasks.

More importantly, owing to the intrinsic coupling between audio and visual modalities in audio-visual foundation models, modifications to the visual stream conditioned on textual prompts inherently propagate to the audio domain. Our proposed method not only synthesizes speech that aligns with attributes such as age, gender, identity, and emotion, but also effectively generates non-linguistic sounds, including children crying or laughing and car engine sounds or sirens. We refer readers to the github page for a comprehensive evaluation of the generated audio quality and cross-modal consistency.

Despite its promising performance, OmniEdit has several limitations in audio-visual editing. It currently struggles with global scene modifications and large-scale style transformations, and may occasionally introduce audio artifacts or background noise, partly due to limitations of the underlying audio-visual foundation model. Nevertheless, the framework is model-agnostic and is expected to benefit from future advances in audio-visual models, enabling broader and higher-quality editing capabilities.

## 6 Conclusion

In this paper, we introduce OmniEdit, a training-free framework for lip synchronization and audio-visual editing. By reformulating the editing process and replacing the edit sequence with the target sequence in the FlowEdit paradigm, the proposed method enables an unbiased estimation of the desired output. Furthermore, by eliminating stochastic components from the generation procedure, OmniEdit establishes a smooth and stable editing trajectory, improving stability and generation quality. Extensive experiments demonstrate that our approach achieves strong performance and robustness across diverse scenarios, validating the effectiveness of the proposed design. We believe this training-free formulation provides a practical and efficient alternative to conventional fine-tuning-based editing methods.

## References

1. Chen, L., Ma, T., Liu, J., Li, B., Chen, Z., Liu, L., He, X., Li, G., He, Q., Wu, Z.: Humo: Human-centric video generation via collaborative multi-modal conditioning (2025), <https://arxiv.org/abs/2509.08519> 3, 10
2. Cheng, K., Cun, X., Zhang, Y., Xia, M., Yin, F., Zhu, M., Wang, X., Wang, J., Wang, N.: Videoretalking: Audio-based lip synchronization for talking head video editing in the wild. In: SIGGRAPH Asia. pp. 30:1–30:9 (2022) 3
3. Cui, J., Li, H., Yao, Y., Zhu, H., Shang, H., Cheng, K., Zhou, H., Zhu, S., Wang, J.: Hallo2: Long-duration and high-resolution audio-driven portrait image animation. In: Int. Conf. Learn. Represent. (2025) 3
4. Fu, Y., Si, R., Wang, H., Zhou, D., Sun, J., Luo, P., Hu, D., Zhang, H., Li, X.: Object-avedit: An object-level audio-visual editing model (2025), <https://arxiv.org/abs/2510.00050> 1
5. Gan, Q., Yang, R., Zhu, J., Xue, S., Hoi, S.: Omniavatar: Efficient audio-driven avatar video generation with adaptive body animation (2025), <https://arxiv.org/abs/2506.18866> 3
6. Gao, X., Hu, L., Hu, S., Huang, M., Ji, C., Meng, D., Qi, J., Qiao, P., Shen, Z., Song, Y., Sun, K., Tian, L., Wang, G., Wang, Q., Wang, Z., Xiao, J., Xu, S., Zhang, B., Zhang, P., Zhang, X., Zhang, Z., Zhou, J., Zhuo, L.: Wan-s2v: Audio-driven cinematic video generation (2025), <https://arxiv.org/abs/2508.18621> 3
7. Goodfellow, I., Pouget-Abadie, J., Mirza, M., Xu, B., Warde-Farley, D., Ozair, S., Courville, A., Bengio, Y.: Generative adversarial networks. *Commun. ACM* **63**(11), 139–144 (2020) 3
8. Guan, K., Wang, X., Lai, Z., Cheng, X., Zhang, P., Liu, X., Song, R., Cao, M.: Taming text-to-sounding video generation via advanced modality condition and interaction (2025), <https://arxiv.org/abs/2510.03117> 3
9. HaCohen, Y., Brazowski, B., Chiprut, N., Bitterman, Y., Kvochko, A., Berkowitz, A., Shalem, D., Lifschitz, D., Moshe, D., Porat, E., Richardson, E., Shiran, G., Chachy, I., Chetboun, J., Finkelson, M., Kupchick, M., Zabari, N., Guetta, N., Kotler, N., Bibi, O., Gordon, O., Panet, P., Benita, R., Armon, S., Kulikov, V., Inger, Y., Shiftan, Y., Melumian, Z., Farbman, Z.: LTX-2: efficient joint audio-visual foundation model, <https://arxiv.org/abs/2601.03233> 3, 10

10. Hertz, A., Aberman, K., Cohen-Or, D.: Delta denoising score. In: Int. Conf. Comput. Vis. pp. 2328–2337 (2023) [3](#)
11. Hertz, A., Mokady, R., Tenenbaum, J., Aberman, K., Pritch, Y., Cohen-Or, D.: Prompt-to-prompt image editing with cross-attention control. In: Int. Conf. Learn. Represent. (2023) [3](#)
12. Ho, J., Jain, A., Abbeel, P.: Denoising diffusion probabilistic models. In: Adv. Neural Inform. Process. Syst. (2020) [2](#)
13. Ji, X., Hu, X., Xu, Z., Zhu, J., Lin, C., He, Q., Zhang, J., Luo, D., Chen, Y., Lin, Q., Lu, Q., Wang, C.: Sonic: Shifting focus to global audio perception in portrait animation. In: IEEE Conf. Comput. Vis. Pattern Recog. pp. 193–203 (2025) [3](#)
14. Kim, J., Hong, Y., Ye, J.C.: Flowalign: Trajectory-regularized, inversion-free flow-based image editing (2025), <https://arxiv.org/abs/2505.23145> [3](#), [5](#)
15. Kim, J., Park, G.Y., Ye, J.C.: Dream sampler: Unifying diffusion sampling and score distillation for image manipulation. In: Eur. Conf. Comput. Vis. vol. 15140, pp. 398–414 (2024) [3](#)
16. Koo, J., Park, C., Sung, M.: Posterior distillation sampling. In: IEEE Conf. Comput. Vis. Pattern Recog. pp. 13352–13361 (2024) [3](#)
17. Kulikov, V., Kleiner, M., Huberman-Spiegelglas, I., Michaeli, T.: Flowedit: Inversion-free text-based editing using pre-trained flow models. In: Int. Conf. Comput. Vis. pp. 19721–19730 (2025) [2](#), [3](#), [4](#), [5](#), [7](#)
18. Li, C., Zhang, C., Xu, W., Lin, J., Xie, J., Feng, W., Peng, B., Chen, C., Xing, W.: Latentsync: Taming audio-conditioned latent diffusion models for lip sync with syncnet supervision (2024), <https://arxiv.org/abs/2412.09262> [1](#), [3](#), [10](#), [11](#)
19. Li, G., Yang, Y., Song, C., Zhang, C.: Flowdirector: Training-free flow steering for precise text-to-video editing, <https://arxiv.org/abs/2506.05046> [3](#)
20. Liang, S., Huang, C., Tian, Y., Kumar, A., Xu, C.: Language-guided joint audio-visual editing via one-shot adaptation. In: Asian Conf. Comput. Vis. vol. 15477, pp. 123–139 (2024) [1](#)
21. Lin, Y., Lin, K., Yang, Z., Li, L., Wang, J., Lin, C., Wang, X., Bertasius, G., Wang, L.: Zero-shot audio-visual editing via cross-modal delta denoising (2025), <https://arxiv.org/abs/2503.20782> [1](#)
22. Lipman, Y., Chen, R.T.Q., Ben-Hamu, H., Nickel, M., Le, M.: Flow matching for generative modeling. In: Int. Conf. Learn. Represent. (2023) [2](#), [4](#)
23. Liu, X., Gong, C., Liu, Q.: Flow straight and fast: Learning to generate and transfer data with rectified flow. In: Int. Conf. Learn. Represent. (2023) [4](#)
24. Low, C., Wang, W., Katyal, C.: Ovi: Twin backbone cross-modal fusion for audio-video generation (2025), <https://arxiv.org/abs/2510.01284> [3](#)
25. Ma, J., Wang, S., Yang, J., Hu, J., Liang, J., Lin, G., Chen, J., Li, K., Meng, Y.: Sayanything: Audio-driven lip synchronization with conditional video diffusion (2025), <https://arxiv.org/abs/2502.11515> [3](#)
26. Ma, Y., Wang, S., Hu, Z., Fan, C., Lv, T., Ding, Y., Deng, Z., Yu, X.: Styletalk: One-shot talking head generation with controllable speaking styles. In: AAAI. pp. 1896–1904 (2023) [3](#)
27. Mantering, H., Huang, Z., Prugel-Bennett, A.: Noise-level diffusion guidance: Well begun is half done (2025), <https://arxiv.org/abs/2509.13936> [7](#)
28. Meng, R., Wang, Y., Wu, W., Zheng, R., Li, Y., Ma, C.: Echomimicv3: 1.3b parameters are all you need for unified multi-modal and multi-task human animation. In: AAAI (2025) [3](#)
29. Mukhopadhyay, S., Suri, S., Gadde, R.T., Shrivastava, A.: Diff2lip: Audio conditioned diffusion models for lip-synchronization. In: IEEE Conf. Win. Appli. Comput. Vis. pp. 5292–5302 (2024) [10](#), [11](#)

30. Nam, H., Kwon, G., Park, G.Y., Ye, J.C.: Contrastive denoising score for text-guided latent diffusion image editing. In: IEEE Conf. Comput. Vis. Pattern Recog. pp. 9192–9201 (2024) [3](#)
31. Peng, Z., Liu, J., Zhang, H., Liu, X., Tang, S., Wan, P., Zhang, D., Liu, H., He, J.: Omnisync: Towards universal lip synchronization via diffusion transformers. In: Adv. Neural Inform. Process. Syst. (2025) [1](#), [3](#), [10](#), [11](#)
32. Podell, D., English, Z., Lacey, K., Blattmann, A., Dockhorn, T., Müller, J., Penna, J., Rombach, R.: SDXL: improving latent diffusion models for high-resolution image synthesis. In: Int. Conf. Learn. Represent. (2024) [2](#)
33. Prajwal, K.R., Mukhopadhyay, R., Namboodiri, V.P., Jawahar, C.V.: A lip sync expert is all you need for speech to lip generation in the wild. In: ACM Int. Conf. Multimedia. pp. 484–492 (2020) [1](#), [3](#), [10](#), [11](#)
34. Rombach, R., Blattmann, A., Lorenz, D., Esser, P., Ommer, B.: High-resolution image synthesis with latent diffusion models. In: IEEE Conf. Comput. Vis. Pattern Recog. (2022) [2](#)
35. Samuel, D., Meiri, B., Maron, H., Tewel, Y., Darshan, N., Avidan, S., Chechik, G., Ben-Ari, R.: Lightning-fast image inversion and editing for text-to-image diffusion models. In: Int. Conf. Learn. Represent. (2025) [3](#)
36. Su, S., Yan, Q., Zhu, Y., Zhang, C., Ge, X., Sun, J., Zhang, Y.: Blindly assess image quality in the wild guided by a self-adaptive hyper network. In: IEEE Conf. Comput. Vis. Pattern Recog. pp. 3664–3673 (2020) [12](#)
37. Team, K.: kling ai (2026), <https://app.klingai.com/> [12](#)
38. Tian, L., Wang, Q., Zhang, B., Bo, L.: EMO: emote portrait alive generating expressive portrait videos with audio2video diffusion model under weak conditions. In: Eur. Conf. Comput. Vis. vol. 15141, pp. 244–260 (2024) [3](#)
39. Tumanyan, N., Geyer, M., Bagon, S., Dekel, T.: Plug-and-play diffusion features for text-driven image-to-image translation. In: IEEE Conf. Comput. Vis. Pattern Recog. pp. 1921–1930 (2023) [3](#)
40. Wallace, B., Gokul, A., Naik, N.: Edict: Exact diffusion inversion via coupled transformations. In: IEEE Conf. Comput. Vis. Pattern Recog. (2023) [3](#)
41. Wang, J., Qian, X., Zhang, M., Tan, R.T., Li, H.: Seeing what you said: Talking face generation guided by a lip reading expert. In: IEEE Conf. Comput. Vis. Pattern Recog. pp. 14653–14662 (2023) [3](#)
42. Wang, Y., Wang, Z., Chen, L.: Target-aware image editing via cycle-consistent constraints (2025), <https://arxiv.org/abs/2510.20212> [7](#)
43. Zhang, Y., Liu, M., Chen, Z., Wu, B., Zeng, Y., Zhan, C., He, Y., Huang, J., Zhou, W.: Musetalk: Real-time high quality lip synchronization with latent space inpainting (2024), <https://arxiv.org/abs/2410.10122> [1](#), [3](#), [10](#), [11](#)
44. Zhang, Z., Li, L., Ding, Y., Fan, C.: Flow-guided one-shot talking face generation with a high-resolution audio-visual dataset. In: IEEE Conf. Comput. Vis. Pattern Recog. pp. 3661–3670 (2021) [11](#)
45. Zhong, W., Fang, C., Cai, Y., Wei, P., Zhao, G., Lin, L., Li, G.: Identity-preserving talking face generation with landmark and appearance priors. In: IEEE Conf. Comput. Vis. Pattern Recog. pp. 9729–9738 (2023) [10](#), [11](#)